

$$v_J^2 = \frac{g_2 v_1^2}{\gamma M_1^2 g_2 + 1} \frac{(1 + 1/\gamma M_1^2)(1 + \gamma M_1^2)}{g_2 + 1} = \frac{hp}{h\rho - p} \quad (9)$$

M_1 and γ do not appear in this equation; the velocity v_J thus depends entirely on the properties of the plasma at this point, regardless how this point was reached. We therefore can drop the index on the right.

On the other hand, a relationship between v_J and the local speed of sound v_s can be established, employing the definition for the Jouguet point,

$$d(j^2)/dp_2 = 0, \quad (10)$$

which means that j^2 has the smallest possible value for the given W . After eliminating v_1 and v_2 from (4) and (5), we differentiate these equations with respect to p_2 , V_2 , h_2 , and j , regarding p_1 , V_1 , h_1 , W as constants,

$$dp_2 + j^2 dV_2 = (V_1 - V_2) d(j^2),$$

$$dh_2 + j^2 V_2 dV_2 = \frac{1}{2}(V_1^2 - V_2^2) d(j^2) - (W/2j^3) d(j^2).$$

Employing $dh_2 = du_2 + p_2 dV_2 + V_2 dp_2$, we eliminate dV_2 and dh_2 ,

$$1 - \frac{j^2 du_2}{p_2 dp_2} = \left(V_1 - V_2 + \frac{W}{2jp_2} - \frac{j^2(V_1 - V_2)^2}{2p_2} \right) \frac{d(j^2)}{dp_2}.$$

The Jouguet point condition (10) then leads to

$$1 = \frac{j^2 du_J}{p_J dp_J} = -\frac{v_J^2}{v_s^2} \frac{1}{p_J} \left(\frac{\partial u_J}{\partial V_J} \right)_s.$$

The internal energy u in a plasma is defined by³

$$du = T dS - p dV + \sum_k \mu_k dc_k,$$

where μ_k is the chemical potential and $c_k = \rho_k/\rho$, the concentration of the k th component. Thus we get

$$v_s = v_J \left(1 - \frac{1}{p_J} \sum_k \mu_k \frac{dc_k}{dV_J} \right)^{\frac{1}{2}}, \quad (11)$$

which gives the well-known relationship $v_s = v_J$ for a nonreacting gas ($dc_k = 0$). In a plasma, v_s will generally differ from v_J . The difference can be evaluated if the gas is specified.

Figure 1 shows examples. Values for the speed of sound were taken from Refs. 1, 12, and 13. v_J was calculated according to this approximation with data from Ref. 1 (argon) and Ref. 5 (hydrogen). It will be noted that v_s oscillates across v_J and differs at most by 12%. Similarly, v_s and v_J in nitrogen⁷ at 1 atm differ by not more than 10%. We therefore

approximate $v_s \approx v_J$ and obtain (2). The advantage of this approximate relationship is that no differentiation is necessary and that h and ρ are available in many cases. For convenience, the approximate speed of sound for oxygen and air (data⁵) is given in Fig. 1.

The author gratefully acknowledges discussion of this topic with Dr. F. L. Curzon, Dr. M. Salvat, and Dr. Wienecke. Dr. Curzon also made valuable comments on the manuscript. The author also wishes to thank Dr. Knoche, who made available numerical data for argon plasma in addition to Ref. 1, and Dr. W. Feneberg at the Institut für Plasmaphysik Garching, who calculated h , $\rho(p, T)$ for helium.

The work was supported by a research grant from the Atomic Energy Control Board of Canada.

¹ F. Bosnjakovic, W. Springs, and K. F. Knoche, *Z. Flugwissensch.* **10**, 413 (1962).

² K. S. Drellishak, C. F. Knopp, and A. B. Cambel, *Phys. Fluids* **6**, 1280 (1963).

³ W. Finkelburg and H. Maecker, in *Handbuch der Physik*, S. Flügge, Ed. (Springer-Verlag, Berlin, 1956), Vol. 22.

⁴ J. Artmann, *Z. Physik* **183**, 65 (1965).

⁵ F. Burhorn and R. Wienecke, in *Landolt-Börnstein*, K. H. Hellwege, Ed. (Springer-Verlag, Berlin, 1961), Bd. II 4, p. 717.

⁶ R. Kuthe and Kl. K. Neumann, *Ber. Bundengesellsch. Physik. Chem.* **68**, 692 (1964).

⁷ K. S. Drellishak, D. P. Aeschilman, and A. B. Cambel, *Phys. Fluids* **8**, 1590 (1965).

⁸ Yu. P. Lun'kin, *Zh. Techn. Fiz.* **29** (1959) [English transl.: *Soviet Phys.—Tech. Phys.* **4**, 155 (1959)].

⁹ B. Ahlborn and M. Salvat, Institut für Plasmaphysik Garching Internal Report IPP 3/2 (1962).

¹⁰ B. Ahlborn, Ph.D. thesis, Technische Hochschule, Munich (1964).

¹¹ L. D. Landau and E. Lifschitz, *Fluid Mechanics* (Pergamon Press, Inc., New York, 1959).

¹² A. B. Cambel, *Plasma Physics and Magnetofluid Mechanics* (McGraw-Hill Book Company, Inc., New York, 1963).

¹³ W. J. Lick and H. W. Emmons, *Thermodynamic Properties of Helium* (Harvard University Press, Cambridge, Massachusetts, 1962).

Experimentally Measured Velocity Distribution in the Plasma Stream of a Pulsed Coaxial Accelerator

T. W. KARRAS, B. GOROWITZ, AND P. GLOERSEN

General Electric Space Sciences Laboratory,
King of Prussia, Pennsylvania

(Received 28 March 1966; final manuscript
received 10 June 1966)

Measurements of the ion velocity distribution in a pulsed plasma stream have been performed. Agreement was found with the average velocity as computed from momentum transfer and mass flow measurements.

THE plasma exhaust from a repetitively pulsed coaxial plasma accelerator for xenon¹ has been investigated by the use of a multigridded particle

analyzer. The specific characteristics sought were: an identification of the multiply ionized accelerated species, a determination of the velocity distribution of the incident ions, and a measure of these characteristics at different positions so that a velocity distribution could be obtained for the entire cross-section of the beam. All this was accomplished by applying different stopping potentials to the grids of the probe to determine particle energy and observing the time-of-flight of the ions that got through to determine particle velocity.

The electrostatic gridded probe used for these observations is similar to that used by Bridge² and Eubank³ but was independently designed. The only significant structural change was in the collector which contained a reentrant cone to minimize the loss of secondary electrons. The other design parameters, mesh size (200 lines/in.) and grid spacing (1/16 in.), were fixed so that Debye shielding and space charge effects^{4,5} were not important.

When the difference is taken between currents to the collector obtained with different ion stopping potentials, this difference represents ions with an energy in the range set by the voltage interval (or some integral multiple of this voltage if the ions are multiply ionized). Since the energy of these ions is well defined, their time-of-flight and velocity should be also, and their velocity distribution can be expressed as

$$f(v) \equiv \frac{dn}{dv} = \frac{dn}{dt} \frac{dt}{dv} = -\frac{I}{ze} \frac{t^2}{d}, \quad (1)$$

where I is the difference between ion currents, z is the number of charges per ion, $v = d/t$ is the velocity of the particles arriving at the probe at a time t , and d is the distance to the probe from the accelerator muzzle.

This equation may be applied to a group of ions with an energy,

$$\frac{1}{2}mv^2 = ze(V_0 \pm \sigma V). \quad (2)$$

By arbitrarily assuming $z = 1$ and plotting $f(v)$ vs v on a graph, the singly ionized particles will be represented by one peak, the doubly ionized by another, etc., since

$$v(z, m) = \frac{d}{t} \cong \left(\frac{2zeV_0}{m} \right)^{\frac{1}{2}}; \quad z = 1, 2, \text{ etc.}, \quad (3)$$

assuming, also, that all particles have the same mass. (Different mass particles will appear in their own peaks.) However, the ordinates of the peaks corresponding to multiply charged ions will be too high by a factor z . Since the real value of z for each peak is then known, a new and correct graph of $f(v)$ vs v may be drawn for this group of ions.

Since the ions do not leave the accelerator at the

instant of discharge initiation, which is time zero for the oscilloscope, some average time lapse may be determined from the correction that must usually be applied to bring $\frac{1}{2}mv^2$ from the time-of-flight into agreement with the zeV characteristic of the voltage interval. This time is a couple of microseconds less than the duration of the current waveform of the accelerator discharge (11 μ sec) when one considers the arrival time of the bulk of the ions. The time lapse was only one or two microseconds for any fast ions ($v \lesssim 10^5$ m/sec). This last group has been interpreted as being ions created and accelerated near the accelerator muzzle during the first few microseconds of discharge.

Velocity distribution plots were obtained by the procedure prescribed in Eq. (1) for ions in various small energy intervals intercepted by the probe while in a given position. Two such distribution plots are shown in Fig. 1. The sum of eight such distributions (with V_0 up to 2.5 kV) gave a total velocity distribution for all the ions in that part of the beam (Fig. 2).

Some dn/dv vs v peaks were observed for particles other than xenon. It is interesting to observe the carbon, oxygen, and hydrogen peaks in Fig. 1. It is expected that these ions resulted from pump oil broken up and accelerated in the plume of the discharge. The low energies involved tend to substantiate this expectation since the acceleration must then have taken place in regions of low current. Despite the seemingly large numbers of particles involved, their atomic weight is so low that their impulse contribution is negligible.

Some dn/dv vs v peaks were observed for particles other than xenon. It is interesting to observe the carbon, oxygen, and hydrogen peaks in Fig. 1. It is expected that these ions resulted from pump oil broken up and accelerated in the plume of the discharge. The low energies involved tend to substantiate this expectation since the acceleration must then have taken place in regions of low current. Despite the seemingly large numbers of particles involved, their atomic weight is so low that their impulse contribution is negligible.

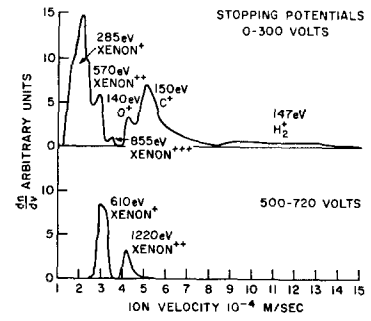
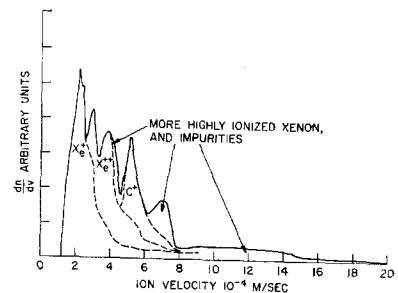


FIG. 2. Total velocity distribution function for all ions passing an on axis probe position 2 m beyond accelerator muzzle plane. The same accelerator operating conditions were used as in Fig. 1. Note the presence of carbon impurities.



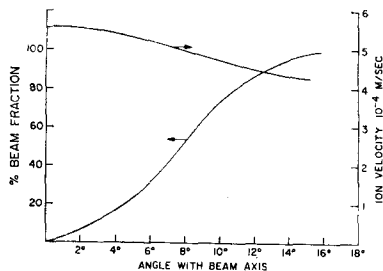


FIG. 3. Fraction of beam ions within a given angle and average ion velocity as function of angle with beam axis. Based upon measurements 2 m beyond accelerator muzzle and operating conditions of Fig. 1.

The average velocity for all ions at this position can be obtained by graphical integration. The average velocity computed for the data in Fig. 2 is 5.2×10^4 m/sec, which corresponds to 1800 eV per particle.

With the limited data on hand, we have found that identical detailed results are not always obtained when the same operating conditions are used at a different time. The most striking difference that occurs is the near absence of the carbon ion peak. All other peaks can be clearly identified. The high energy tail and the relative heights of the various xenon peaks are also different. In spite of these differences, the average velocity obtained from such a distribution function is 5.55×10^4 m/sec, within 7% of the other value, and well within the estimated experimental error of $\pm 20\%$.

Essentially the same results were obtained when the probe was moved 43 cm off-axis in the same plane 2 m downstream from the muzzle. Data were obtained also at a number of intermediate radial points to permit determination of the distribution function and the average ion velocity as a function of radius.

From an integration of this data, the fraction of the ions within a radius R and the average ion velocity, \bar{v} , have been determined and are shown in Fig. 3 as function of angle with the beam axis.

Using this knowledge of \bar{v} across the beam, the average velocity of all ions in the exhaust was obtained. This was found to be 5.3×10^4 m/sec when the accelerator was operating under the same conditions as those above. However, it is important to note that since about 10% of the injected propellant was not acted upon by the discharge,¹ and so emerges as un-ionized gas, the average velocity of all the exhaust is about 4.75×10^4 m/sec.

As an independent check of this number, the average reactive force on the accelerator and the injected gross mass flow were measured.¹ The average exhaust velocity as determined by this technique was 4.8×10^4 m/sec, in excellent agreement with the average velocity as determined by the probe. It should be emphasized that this close correspondence is at least in part fortuitous since the estimated errors are so large.

This work was sponsored by the National Aeronautics and Space Administration, Contract NASw-1044.

¹ B. Gorowitz, P. Gloersen, and T. W. Karras, AIAA J. (to be published).

² H. S. Bridge, C. Dilworth, B. Rossi, F. Scherb, and E. F. Lyon, J. Geophys. Res. **65**, 3053 (1960); **68**, 4017 (1963).

³ H. E. Eubank, Bull. Am. Phys. Soc. **10**, 219 (1965).

⁴ H. A. Fleishmann, D.E.T.F. Ashby, and A. V. Larson, Nucl. Fusion **5**, 394 (1965).

⁵ B. Salzberg and A. V. Haeff, RCA Rev. **2**, 336 (1937).

Turbulent Magnetohydrodynamic Channel Flow

H. TENNEKES

*Department of Aeronautical Engineering,
The Pennsylvania State University,
University Park, Pennsylvania*

(Received 16 December 1965; final manuscript received 6 July 1966)

An analogy appears to exist between turbulent magnetohydrodynamic channel flow at high Reynolds numbers and moderate Hartmann numbers on one hand, and turbulent boundary-layer flow with suction on the other. Skin-friction calculations confirm the existence of the analogy.

IT is well known that a transverse magnetic field tends to inhibit turbulent fluctuations in the flow of a conducting fluid. Data obtained by Hartmann and Lazarus,¹ Murgatroyd,² and Branover and Lielausis³ indicate that, at sufficiently large Hartmann numbers, turbulent motion will be suppressed completely. The turbulence-suppression effect is strong at low Reynolds numbers ($R < 10^3$), but it seems to be absent at sufficiently high Reynolds numbers (Brouillette and Lykoudis⁴). This conclusion is in agreement with evidence obtained by Globe,⁵ showing that an axial magnetic field (which does not produce a Hartmann effect) is unable to suppress turbulence if the Reynolds number is high enough. A review of the double role of a transverse magnetic field (suppression of turbulence versus Hartmann effect) has recently been given by Branover and Lielausis.⁶ They suggest that for Reynolds numbers sufficiently far beyond the transition range "laminarization occurs, not due to the direct effect of the field on the pulsations, but owing to a flattening of the mean velocity profiles."

Some years ago, Lykoudis⁷ suggested that turbulent hydromagnetic channel flow bears a close resemblance to turbulent boundary-layer flow with suction. The analogy is based on the similarity of the mean velocity profiles of the viscous sublayers in the respective flows. This paper is devoted to a further evaluation of the analogy. For this purpose, skin-friction coefficients for hydromagnetic channel flow are calculated, using experimental data ob-